Isospecific Propylene Polymerization by C_1-Symmetric $Me_2Si(C_5Me_4)(2\text{-R-Ind})MCl_2$ (M = Ti, Zr) Complexes

Min Hyung Lee, Yonggyu Han, Do-hyeon Kim, Jeong-Wook Hwang, and Youngkyu Do*

Department of Chemistry, School of Molecular Science-BK21 and Center for Molecular Design and Synthesis, Korea Advanced Institute of Science and Technology, Daejeon 305-701, Republic of Korea

Received August 29, 2002

Novel C_1-symmetric group 4 *ansa*-metallocene complexes $Me_2Si(C_5Me_4)(2\text{-R-Ind})MCl_2$ (R = H, M = Ti (**5a**), Zr (**5b**); R = Me, M = Ti (**6a**), Zr (**6b**)) were prepared from the reaction of dilithium salt of the corresponding ligands $Me_2Si(C_5Me_4H)(2\text{-R-IndH})$ (R = H, Me) with appropriate group 4 metal halides. Crystal structures of **5a**, **6a**, and **6b** determined by X-ray diffraction studies reveal chiral C_1-symmetric nature irrespective of the type of metal and ligand. The complexes **5a**, **5b**, **6a**, and **6b** were tested for the polymerization of propylene in the presence of methylaluminoxane (MAO) at various temperatures. All of them exhibit good activity and afford moderate to high isotactic polypropylenes. In the case of titanocenes (**5a** and **6a**), polymerization activity, molecular weight, and isotacticity of polypropylene sharply increase as the polymerization temperature decreases, while the increase of polymerization activity and the decrease of isotacticity and molecular weight of polypropylene were observed upon increasing the polymerization temperature in the case of zirconocenes (**5b** and **6b**). The effect of a 2-Me substituent at the indenyl ring on propylene polymerization was apparent in terms of polymerization activity and molecular weight of polypropylene, especially for zirconocenes, but was minor for titanocenes.

Downloaded by CARLI CONSORTIUM on June 29, 2009
Published on May 24, 2003 on http://pubs.acs.org | doi: 10.1021/om020712t

Introduction

Single-site catalytic systems based on group 4 metallocene complexes have been extensively investigated as catalysts for the polymerization of ethylene and α-olefins during the recent two decades.[1] In particular, the studies on the stereospecific polymerization of propylene have been well established in such a way that highly isotactic polypropylene (iPP)[2] and syndiotactic polypropylene (sPP)[3] could be tailored by means of C_2- and C_s-symmetric *ansa*-metallocene complexes, respectively. Along with these highly stereospecific metallocene complexes, but to a lesser extent, asymmetric C_1-symmetric metallocenes have also been developed to produce polypropylene with microstructure varying from hemiisotatic[4] to stereoblock[5] to isotatic.[6] Moreover, synthetic advantages such as the formation of a single metallocene isomer and the easy variation of ligand framework depending on the substituent on the cyclopentadienyl ring fragments made C_1-symmetric catalysts of potentially great interest in new polymer synthesis.

Chien et al. first introduced the C_1-symmetric monocarbon-bridged complex $[MeHC(C_5Me_4)(Ind)]TiCl_2$ (**1** in Figure 1), which produces thermoplastic elastic polypropylene having isotactic−atactic stereoblock sequences.[5a−d] Chien's zirconium analogue of **1**, on the contrary, affords hemiisotactic polypropylene in low yield.[4c] Along the same line, Collins et al. reported catalysts (**2**) similar to Chien's system, but lacking any substituent on the cyclopentadienyl ring, to give elastomeric polypropylene.[5e] In this case, both the monocarbon- and silicon-bridged complexes of hafnium operate better than zirconium

* To whom correspondence should be addressed. Fax: +82-42-869-2810. E-mail: ykdo@kaist.ac.kr.

(1) For recent reviews of group 4 metallocene catalysts, see: (a) Brintzinger, H. H.; Fischer, D.; Mülhaupt, R.; Rieger, B.; Waymouth, R. M. *Angew. Chem., Int. Ed. Engl.* **1995**, *34*, 1143. (b) Bochmann, M. *J. Chem. Soc., Dalton Trans.* **1996**, *255*. (c) Resconi, L.; Cavallo, L.; Fait, A.; Piemontesi, F. *Chem. Rev.* **2000**, *100*, 1253.

(2) (a) Ewen, J. A. *J. Am. Chem. Soc.* **1984**, *106*, 6355. (b) Kaminsky, W.; Kulper, K.; Brintzinger, H. H.; Wild, F. R. W. P. *Angew. Chem., Int. Ed. Engl.* **1985**, *24*, 507.

(3) (a) Ewen, J. A.; Jones, R. L.; Razavi, A.; Ferrara, J. D. *J. Am. Chem. Soc.* **1988**, *110*, 6255. (b) Ewen, J. A.; Elder, M. J.; Jones, R. L.; Curtis, S.; Cheng, H. N. In *Catalytic Olefin Polymerization*; Keii, T., Soga, K., Eds.; Elsevier: New York, 1990; pp 439−482.

(4) (a) Fierro, R.; Chien, J. C. W.; Rausch, M. D. *J. Polym. Sci. Part A: Polym. Chem.* **1994**, *32*, 2817. (b) Guerra, G.; Cavallo, L.; Moscardi, G.; Vacatello, M.; Corradini, P. *Macromolecules* **1996**, *29*, 4834. (c) Llinas, G. H.; Day, R. O.; Rausch, M. D.; Chien, J. C. W. *Organometallics* **1993**, *12*, 1283.

(5) (a) Mallin, D. T.; Rausch, M. D.; Lin, Y.-G.; Dong, S.; Chien, J. C. W. *J. Am. Chem. Soc.* **1990**, *112*, 2030. (b) Chien, J. C. W.; Llinas, G. H.; Rausch, M. D.; Lin, Y.-G.; Winter, H. H.; Atwood, J. L.; Bott, S. G. *J. Am. Chem. Soc.* **1991**, *113*, 8569. (c) Llinas, G. H.; Dong, S.-H.; Mallin, D. T.; Rausch, M. D.; Lin, Y.-G.; Winter, H. H.; Chien, J. C. W. *Macromolecules* **1992**, *25*, 1242. (d) Babu, G. N.; Newmark, R. A.; Cheng, H. N.; Llinas, G. H.; Chien, J. C. W. *Macromolecules* **1992**, *25*, 7400. (e) Gauthier, W. J.; Corrigan, J. F.; Taylor, N. J.; Collins, S. *Macromolecules* **1995**, *28*, 3771. (f) Gauthier, W. J.; Collins, S. *Macromolecules* **1995**, *28*, 3779. (g) Bravakis, A. M.; Bailey, L. E.; Pigeon, M.; Collins, S. *Macromolecules* **1998**, *31*, 1000.

(6) (a) Thomas, E. J.; Chien, J. C. W.; Rausch, M. D. *Macromolecules* **2000**, *33*, 1546. (b) Thomas, E. J.; Rausch, M. D.; Chien, J. C. W. *Organometallics* **2000**, *19*, 4077. (c) Kukral, J.; Lehmus, P.; Feifel, T.; Troll, C.; Rieger, B. *Organometallics* **2000**, *19*, 3767. (d) Dietrich, U.; Hackmann, M.; Rieger, B.; Klinga, M.; Leskelä, M. *J. Am. Chem. Soc.* **1999**, *121*, 4348. (e) Rieger, B.; Gerhard, J.; Fwazi, R.; Steimann, M. *Organometallics* **1994**, *13*, 647. (f) Giardello, M. A.; Eisen, M. S.; Stern, C. L.; Marks, T. J. *J. Am. Chem. Soc.* **1993**, *115*, 3326. (g) Giardello, M. A.; Eisen, M. S.; Stern, C. L.; Marks, T. J. *J. Am. Chem. Soc.* **1995**, *117*, 12114. (h) Miyake, S.; Okumura, Y.; Inazawa, S. *Macromolecules* **1995**, *28*, 3074.

10.1021/om020712t CCC: $25.00 © 2003 American Chemical Society
Publication on Web 05/24/2003

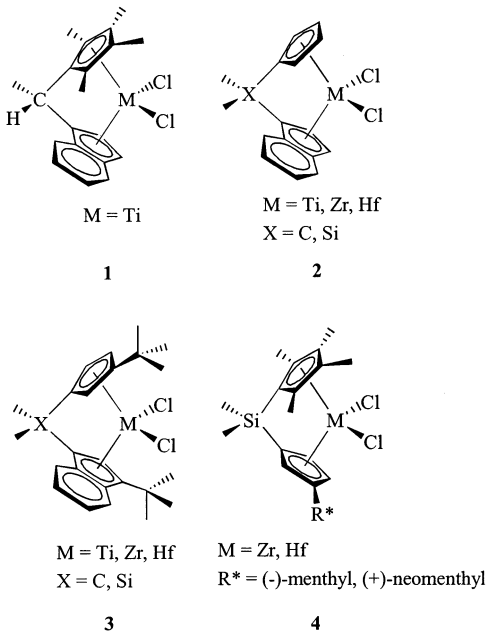

Figure 1. Examples of C_1-symmetric *ansa*-metallocenes.

Downloaded by CARLI CONSORTIUM on June 29, 2009
Published on May 24, 2003 on http://pubs.acs.org | doi: 10.1021/om020712t

complexes. Razavi et al. also demonstrated that the variation of β-substituent on the cyclopentadienyl ring from H to Me and *t*-Bu of the Ewen's C_s-symmetric catalyst *i*-Pr(Flu)(Cp)$ZrCl_2$ resulted in the production of hemiisotactic and isotactic polypropylene, respectively.[7] Highly isotactic polypropylene, which has been believed to be the nearly sole product of C_2-symmetric metallocene complexes, proved to be another major outcome of C_1-symmetric catalytic systems. Miyake's catalyst (**3**)[6h] and Marks' system (**4**)[6f,g] are the best examples that produce highly isotactic polypropylene.

The aforementioned works on C_1-symmetric catalysts clearly indicate that all components constituting metallocene catalytic systems such as a metal ion, a cyclopentadienyl ring, a substituent on the ring, and a bridging group are very important factors in controlling the properties of the resulting polypropylene. In the present paper, we aimed to prepare and characterize a series of C_1-symmetric *ansa*-metallocene complexes containing linked indenyl-tetramethylcyclopentadienyl ligands, which seemingly resemble Chien's catalyst (**1**) except the replacement of a monocarbon bridge with a monosilyl group, to investigate the effects of bridging group, substituent, and metal center on the propylene polymerization reactions.

Experimental Section

General Considerations. All operations were performed under an inert dinitrogen atmosphere using standard Schlenk and glovebox techniques. THF, toluene, and *n*-hexane were distilled from Na−K alloy, Et_2O from Na−benzophenone ketyl, and CH_2Cl_2 from CaH_2. Chemicals were used without any further purification after purchasing from Aldrich ($ZrCl_4$, indene, 2-methylindene, Me_2SiCl_2, *n*-butyllithium (2.5 M solution in *n*-hexane)) and Strem ($Li(C_5Me_4H)$). $Me_2Si(C_5Me_4H)Cl$[8] and $TiCl_4(THF)_2$[9] were prepared according to the literature procedures. $CDCl_3$ was dried over activated molecular sieves (4 Å) and used after vacuum transfer to a Schlenk tube equipped with a J. Young valve. ^1H and ^{13}C NMR spectra of samples except polypropylenes were recorded on a Bruker Avance 300. All chemical shifts are reported in δ units with reference to the residual peaks of $CDCl_3$ for proton (7.24 ppm) and carbon (77.0 ppm) chemical shifts. HR EIMS experiments were performed on a VG Auto Spec at KAIST. Elemental analyses were carried out on an EA 1110-FISONS (CE Instruments) at KAIST and a Carlo Erba EA 1108 at Korea Basic Science Center (KBSC).

Synthesis of $Me_2Si(C_5Me_4H)(IndH)$ (5). A solution of indene (1.16 g, 10.0 mmol) in THF was treated with an equimolar amount of *n*-butyllithium at −78 °C. The reaction mixture was slowly allowed to warm to room temperature by removing the cooling bath and stirred for 2 h at this temperature. Into the precooled flask containing 2.15 g of $Me_2Si(C_5Me_4H)Cl$ (10.0 mmol) in 20 mL of THF was slowly added the solution of indenyllithium via cannula at −78 °C. The reaction mixture was slowly allowed to warm to room temperature and stirred for an additional 6 h at this temperature. The reaction was stopped by the addition of water, and the organic portion was extracted with ether (30 mL × 2). The aqueous layer was further extracted with ether (20 mL), and the combined organics were dried over $MgSO_4$. Filtration and rotary-evaporation of the solvent gave a light brownish residue, which was further purified by column chromatography (silica gel, eluent: hexane), affording 2.75 g (93.0%) of **5** as light yellow-green oil. The product was found to be a mixture of two stereoisomers (1-isomer:3-isomer = 2.2:1) as judged by ^1H NMR spectroscopy. ^1H NMR (300.13 MHz, $CDCl_3$): 1-isomer, δ 7.56−7.53 (m, 2H), 7.33−7.26 (m, 2H), 7.00 (d, 1H), 6.65 (dd, 1H), 3.52 (d, 1H), 3.17 (s, 1H), 1.98 (s, 6H), 1.91 (s, 6H), −0.03 (s, 3H), −0.31 (s, 3H); 3-isomer, δ 7.63−7.57 (m, 2H), 7.39−7.36 (m, 2H), 6.62 (s, 1H), 3.74 (s, 2H), 3.34 (s, 1H), 2.14 (s, 6H), 2.11 (s, 6H), 0.29 (s, 6H). HR EIMS: *m*/*z* calcd for $C_{20}H_{26}Si$, 294.1804; found, 294.1794.

Synthesis of $Me_2Si(C_5Me_4H)(2\text{-}MeIndH)$ (6). The reaction of 2-methylindene (7.0 mmol, 0.91 g) with the same equivalent of $Me_2Si(C_5Me_4H)Cl$ (1.5 g) by a method similar to that described above afforded 1.7 g (78%) of **6** (1-isomer only) as a light yellow oil. ^1H NMR (300.13 MHz, $CDCl_3$): δ 7.39 (d, 1H), 7.30 (d, 1H), 7.18 (dd, 1H), 7.06 (dd, 1H), 6.56 (s, 1H), 3.61 (s, 1H), 3.23 (s, 1H), 2.23 (s, 3H), 2.01 (s, 3H), 1.95 (s, 3H), 1.83 (s, 3H), 1.80 (s, 3H), −0.30 (s, 3H), −0.35 (s, 3H). HR EIMS: *m*/*z* calcd for $C_{21}H_{28}Si$, 308.1960; found, 308.1964.

Synthesis of $Me_2Si(C_5Me_4)(Ind)TiCl_2$ (5a). A solution of **5** (1.3 g, 4.5 mmol) in 40 mL of a mixed solvent of diethyl ether/*n*-hexane (v/v = 1:1) was treated with 2 equiv of *n*-BuLi (3.6 mL) at 0 °C. The reaction mixture was allowed to warm to room temperature and stirred overnight. The light yellow solution over the precipitate was decanted off, and the salt was washed twice with *n*-hexane (20 mL × 2). Drying in vacuo gave a nearly quantitative dilithium salt of **5** as an ivory powder. The dilithium salt obtained was then mixed with an equimolar amount of $TiCl_4(THF)_2$ (1.5 g), and this solid mixture was cooled to −78 °C. Into the cooled flask was added slowly 40 mL of toluene with vigorous stirring. The yellow slurry turned gradually to greenish. After 1 h at −78 °C, the reaction mixture was slowly allowed to warm to room temperature and stirred for 4 h, giving a dark brown-green solution with some precipitate (LiCl). Evaporation of the solvent and extraction of the residue with CH_2Cl_2 (30 mL) followed by filtration through a Celite pad afforded a dark brownish green solution. The reduction of the volume of the filtrate to 20 mL was followed by the addition of *n*-hexane (20 mL) to the concentrated filtrate and cooling to −20 °C overnight, affording 0.50 g of dark greenish microcrystals of **5a** (27%). Single crystals suitable for X-ray diffraction study were obtained by cooling the CH_2Cl_2 solution of **5a** layered by *n*-hexane at −20 °C. ^1H NMR (300.13 MHz, $CDCl_3$): δ 7.65

(7) Razavi, A.; Napfliotis, L.; Peters, L.; Vereecke, D.; Den Dauw, K.; Atwood, J. L.; Thewald, U. *Macromol. Symp.* **1995**, *89*, 345.
(8) Shapiro, P. J.; Cotter, W. D.; Schaefer, W. P.; Labinger, J. A.; Bercaw, J. E. *J. Am. Chem. Soc.* **1994**, *116*, 4623.
(9) Manzer, L. E. *Inorg. Synth.* **1982**, *21*, 135.

Downloaded by CARLI CONSORTIUM on June 29, 2009
Published on May 24, 2003 on http://pubs.acs.org | doi: 10.1021/om020712t

Table 1. Crystallographic Data and Parameters for 5a, 6a, and 6b

	5a	6a	6b
formula	$C_{20}H_{24}SiCl_2Ti$	$C_{21}H_{26}SiCl_2Ti$	$C_{21}H_{26}SiCl_2Zr$
fw	411.28	425.31	468.64
cryst syst	triclinic	monoclinic	monoclinic
space group	$P\bar{1}$	$P2_1/n$	$P2_1/n$
a (Å)	9.659(3)	14.054(3)	14.078(3)
b (Å)	10.470(2)	9.098(1)	9.196(1)
c (Å)	10.597(2)	15.653(2)	15.810(3)
α (deg)	74.35(2)	90	90
β (deg)	74.90(2)	95.55(1)	95.84(2)
γ (deg)	71.19(3)	90	90
V (Å^3)	959.0(4)	1992.0(5)	2036.1(6)
Z	2	4	4
d_{calcd} (g/cm^3)	1.424	1.418	1.529
F(000)	428	888	960
μ(Mo Kα) (mm^{-1})	0.786	0.760	0.863
cell meas 2θ range (deg)	14.80; 27.59	20.69; 29.12	13.61; 27.49
T (K)	293	293	293
scan mode	ω/θ	ω/θ	$\omega/2\theta$
data col θ range (deg)	2.03; 24.97	2.05; 24.98	2.04; 24.97
no. of uniq reflns	2931	3188	2811
no. of obs reflns ($I > 2\sigma(I)$)	2377	2693	1858
no. of params refined	223	229	229
R1[a]	0.0671	0.0719	0.0739
wR2[b]	0.2133	0.1578	0.1404
GOF	1.064	1.340	1.149
min. and max. dens (e Å^{-3})	−0.376; 0.839	−1.862; 1.973	−0.629; 0.636

[a] $R1 = \sum||F_o| - |F_c||/\sum|F_o|$. [b] $wR2 = [\sum[w(F_o^2 - F_c^2)^2]/\sum[w(F_o^2)^2]]^{1/2}$.

Table 2. Selected Interatomic Distances (Å) and Angles (deg) for 5a, 6a, and 6b

	5a (M = Ti)	6a (M = Ti)	6b (M = Zr)
	Angles		
Cl(1)−M−Cl(2)	98.2(1)	96.8(1)	98.9(1)
Cn(1)−M−Cn(2)	131.5	131.4	128.2
C(1)−Si(1)−C(12)	91.3(3)	91.5(2)	94.2(4)
C(10)−Si(1)−C(11)	107.7(4)	104.3(2)	105.1(5)
	Distances		
M−Cl(1)	2.312(2)	2.320(1)	2.420(3)
M−Cl(2)	2.359(2)	2.358(2)	2.440(3)
M−C(1)	2.375(7)	2.378(3)	2.468(8)
M−C(2)	2.347(6)	2.421(5)	2.541(9)
M−C(3)	2.493(6)	2.499(5)	2.608(10)
M−C(8)	2.530(7)	2.483(5)	2.548(10)
M−C(9)	2.652(6)	2.596(5)	2.632(10)
M−C(12)	2.357(6)	2.358(4)	2.459(9)
M−C(13)	2.395(6)	2.401(4)	2.502(10)
M−C(14)	2.516(6)	2.525(5)	2.629(11)
M−C(15)	2.502(6)	2.516(5)	2.604(11)
M−C(16)	2.363(6)	2.400(4)	2.480(10)
M−Cn(1)	2.166(3)	2.158(2)	2.252(4)
M−Cn(2)	2.104(3)	2.119(2)	2.225(5)

[a] Cn(1) and Cn(2) are the centroids of each C_5 ring of the Ind and C_5Me_4 group, respectively.

(d, 1H), 7.52 (d, 1H), 7.40 (dd, 1H), 7.37 (d, 1H), 7.08 (dd, 1H), 5.87 (d, 1H), 2.01 (s, 3H), 1.99 (s, 3H), 1.87 (s, 3H), 1.77 (s, 3H), 1.17 (s, 3H), 0.98 (s, 3H). $^{13}C\{^1H\}$ NMR (75.47 MHz, $CDCl_3$): δ 143.2, 142.2, 137.2, 134.8, 132.1, 130.8, 128.9, 128.7, 127.8, 126.5, 125.1, 117.6, 95.9, 88.3, 16.4, 16.0, 13.7, 13.3, 1.4, 0.5. Anal. Calcd for $C_{20}H_{24}SiCl_2Ti$: C, 58.41; H, 5.88. Found: C, 58.28; H, 6.08.

Synthesis of $Me_2Si(C_5Me_4)(Ind)ZrCl_2$ (5b). The reaction of dilithium salt of **5**, prepared by a procedure similar to that described above (**5**: 3.5 mmol, 1.0 g; *n*-BuLi: 2.8 mL), with

Table 3. Geometrical Parameters (deg or Å) of 5a, 6a, and 6b

	5a (M = Ti)	6a (M = Ti)	6b (M = Zr)
α	131.5	131.4	128.2
β	60.5(4)	58.9(3)	61.2(6)
ϕ	91.3(3)	91.5(2)	94.2(4)
γ_1	14.7(3)	16.7(2)	17.2(5)
γ_2	16.1(3)	16.0(2)	16.1(5)
δ_1	81.5	84.5	85.5
δ_2	84.7	84.4	84.8
d_1(M−Cn)	2.166(3)	2.158(2)	2.252(4)
d_2(M−Cn)	2.104(3)	2.119(2)	2.225(5)

[a] 1 and 2 denote each C_5 ring of the Ind and C_5Me_4 group, respectively. [b] Cn, C_5 ring centroid.

an equimolar amount of $ZrCl_4$ (0.82 g) in toluene (30 mL) at −78 °C resulted in a white slurry, which finally turned to a yellow reaction mixture after stirring for 4 h at room temperature. Removal of the solvent and extraction with CH_2Cl_2 (30 mL) followed by filtration gave a bright yellow solution. The concentrated filtrate was treated with *n*-hexane (20 mL) and stored at −20 °C overnight, giving 0.67 g of **5b** as bright yellow crystals (42%). ^1H NMR (300.13 MHz, $CDCl_3$): δ 7.68 (d, 1H), 7.48 (d, 1H), 7.33 (dd, 1H), 7.21 (d, 1H), 7.05 (dd, 1H), 5.97 (d, 1H), 1.95 (s, 3H), 1.94 (s, 3H), 1.91 (s, 3H), 1.89 (s, 3H), 1.14 (s, 3H), 0.94 (s, 3H). $^{13}C\{^1H\}$ NMR (75.47 MHz, $CDCl_3$): δ 135.8, 135.4, 133.2, 129.0, 128.2, 128.1, 126.8, 126.3, 126.1, 124.9, 120.2, 117.1, 96.8, 88.3, 15.3, 14.9, 12.4, 12.1, 1.2, 1.0. Anal. Calcd for $C_{20}H_{24}SiCl_2Zr$: C, 52.84; H, 5.32. Found: C, 52.45; H, 5.65.

Synthesis of $Me_2Si(C_5Me_4)(2\text{-}MeInd)TiCl_2$ (6a). Following the above procedure for complex **5a** (**6**: 2.7 mmol, 0.83 g; *n*-BuLi: 2.2 mL; $TiCl_4(THF)_2$: 0.90 g) resulted in dark greenish crystals of **6a** (0.29 g, 25%). Single crystals were grown from the CH_2Cl_2 solution of **6a** layered by *n*-hexane at −20 °C. ^1H NMR (300.13 MHz, $CDCl_3$): δ 7.55−7.52 (m, 2H), 7.35 (dd, 1H), 7.13 (s, 1H), 6.92 (dd, 1H), 2.17 (s, 3H), 2.05 (s, 3H), 2.00 (s, 3H), 1.88 (s, 3H), 1.70 (s, 3H), 1.22 (s, 3H), 1.11 (s, 3H). $^{13}C\{^1H\}$ NMR (75.47 MHz, $CDCl_3$): δ 145.6, 141.1, 140.9, 136.6, 135.2, 133.0, 129.9, 128.2, 126.6, 126.5, 125.6, 124.6, 92.4, 84.5, 19.3, 16.9 (2C), 13.7, 13.2, 2.7, 2.6. Anal. Calcd for $C_{21}H_{26}SiCl_2Ti$: C, 59.31; H, 6.16. Found: C, 59.50; H, 6.22.

Synthesis of $Me_2Si(C_5Me_4)(2\text{-}MeInd)ZrCl_2$ (6b). The employment of the procedures for complexes **5a** and **5b** with **6** (**6**: 2.8 mmol, 0.86 g; *n*-BuLi: 2.3 mL; $ZrCl_4$: 0.65 g) resulted in bright yellow crystals of **6b** (0.53 g, 40%). Single crystals were grown from the CH_2Cl_2/*n*-hexane solution of **6b** at −20 °C. ^1H NMR (300.13 MHz, $CDCl_3$): δ 7.59−7.55 (m, 2H), 7.29 (dd, 1H), 6.95 (dd, 1H), 6.91 (s, 1H), 2.29 (s, 3H), 2.06 (s, 3H), 1.96 (s, 3H), 1.86 (s, 3H), 1.85 (s, 3H), 1.17 (s, 3H), 1.07 (s, 3H). $^{13}C\{^1H\}$ NMR (75.47 MHz, $CDCl_3$): δ 138.0, 135.3, 135.2, 129.0, 128.4, 128.2, 127.3, 126.2, 125.5, 125.4, 124.3, 120.0, 94.5, 83.4, 18.3, 15.8, 15.6, 12.4, 12.1, 3.1, 3.0. Anal. Calcd for $C_{21}H_{26}SiCl_2Zr$: C, 53.82; H, 5.59. Found: C, 52.96; H, 5.46.

Propylene Polymerizations. Into a well-degassed 500 mL glass reactor, freshly distilled toluene was transferred via cannula, and then a toluene solution of MMAO (Al/Zr = 2000, Akzo) was syringed into the reactor. Then, the reactor was adjusted to constant temperature (−20, 0, 25, and 50 °C) using an external bath, degassed with propylene several times, and saturated with propylene at 1 bar with vigorous stirring. After presaturation of propylene, polymerization was initiated by injecting a toluene solution of catalyst. Initial color change of the reaction mixture and the rapid consumption of propylene were observed. After the given reaction time (t_p in Table 4), polymerization was quenched by pouring the reaction mixture into 100 mL of 10% HCl solution of MeOH, and the resulting polypropylene was further precipitated by the addition of 300 mL of MeOH. After stirring for 1 h, the solid polypropylene was filtered off, washed with MeOH several times, and then dried under vacuum overnight at 60 °C. Polymer Analysis. ^{13}C

Table 4. Propylene Polymerization Data with Catalysts 5a, 5b, 6a, and 6b/MMAO[a]

entry	catalyst	[cat.] (μmol)	T_p (°C)	t_p (min)	yield (g)	activity[b]	M_w ($\times 10^{-3}$)	M_w/M_n	T_m (°C)	mmmm[c]
1	**5a**	5	25	60	1.223	245	27.1	1.78	116.8	0.717
2	**5a**	5	0	60	4.716	943	209	3.24	132.3	0.827
3	**5a**	1	−20	1.5	2.186	87 440	2,650	1.96	142.7	0.881
4	**5b**	1	50	15	6.672	26 688	30.8	1.78	110.8	0.700
5	**5b**	5	25	30	11.608	4643	52.7	1.79	124.4	0.817
6	**5b**	5	0	30	1.345	538	101	1.74	111.5	0.759
7	**6a**	5	25	60	0.188	38	9.27	1.47	n.d.[d]	0.176
8	**6a**	5	0	60	1.348	270	72.5	1.90	107.6	0.694
9	**6a**	1	−20	1.5	0.638	25 520	797	2.65	146.3	0.911
10	**6b**	1	50	30	5.094	10 188	58.8	1.84	98.5	0.640
11	**6b**	5	25	30	8.811	3524	113	1.83	121.0	0.788
12	**6b**	5	0	30	2.262	905	178	1.95	115.8	0.770

[a] Conditions: *P*(propylene), 1 bar; solvent, 100 mL of toluene; [Al]/[M], 2000. [b] Activity, kgPP/(mol of M)·h·bar. [c] Determined by ^{13}C NMR spectroscopy. [d] n.d., not determined due to viscous oily PP.

NMR spectra of polypropylenes with moderate isotacticity were recorded either on a Bruker AM 300 or on a Bruker Avance 400 spectrometers in 15 wt % polypropylene solutions of *o*-dichlorobenzene (*o*-DCB)/C_6D_6 at 80 °C, and those of the polypropylenes with high isotacticity were recorded on a Bruker AM 500 spectrometer in $C_2D_2Cl_4$ at 120 °C. Molecular weight and molecular weight distribution of polypropylenes were determined by GPC (Waters 150C, 130 °C) in 1,2,4-trichlorobenzene using polystyrene column as a standard. Melting temperatures (T_m) of polypropylenes were measured by differential scanning calorimetry (DSC, TA instruments DSC 2010).

X-ray Structure Determination of 5a, 6a, and 6b. All crystals were mounted on glass capillaries, and diffraction data were collected on an Enraf-Nonius CAD4TSB diffractometer equipped with graphite-monochromated Mo Kα radiation (λ = 0.71073 Å) at 293 K. Accurate unit cell parameters and orientation matrixes were determined from the least-squares fit of 25 accurately centered reflections in the range of 2θ given in Table 1. Intensity data were collected by using the $\omega-\omega$ (for **5a** and **6a**) or $\omega-2\theta$ (for **6b**) scan mode with a range of $2.00° \le \theta \le 25.00°$. All the intensity data were corrected for Lorentz and polarization effects. The structures were solved by a semi-invariant direct method (SIR 92 in MoleN)[10] and refined by full matrix least-squares refinement (SHELXL 93)[11] with anisotropic thermal parameters for all non-hydrogen atoms. Hydrogen atoms were placed at their geometrically calculated positions and refined riding on the corresponding carbon atoms with isotropic thermal parameters. Final refinement was carried out by considering the reflections with $I > 2.0\sigma(I)$. All calculations were performed on a Silicon Graphics Indigo2XZ workstation. The detailed crystallographic data are listed in Table 1.

Downloaded by CARLI CONSORTIUM on June 29, 2009
Published on May 24, 2003 on http://pubs.acs.org | doi: 10.1021/om020712t

Results and Discussion

Synthesis and Crystal Structures. Synthetic routes to monosilyl-bridged ligand systems and their group 4 metal complexes are summarized in Scheme 1. The reactions of $Me_2Si(C_5Me_4H)Cl$ with indenyllithium anions in THF at low temperature afforded the corresponding ligands **5** and **6** in high yields. In contrast to this method, the reactions of Me_2Si(2-R-IndH)Cl (R = Me, H) with Li(C_5Me_4H) in THF failed to produce the desired ligands, although the latter approach was previously adopted by Collins et al. in preparing Me_2Si(CpH)(IndH) from NaCp and Me_2Si(IndH)Cl.[5e] Straightforward metalations were effected by the addition of toluene into the solid mixture of $ZrCl_4$ or

Scheme 1

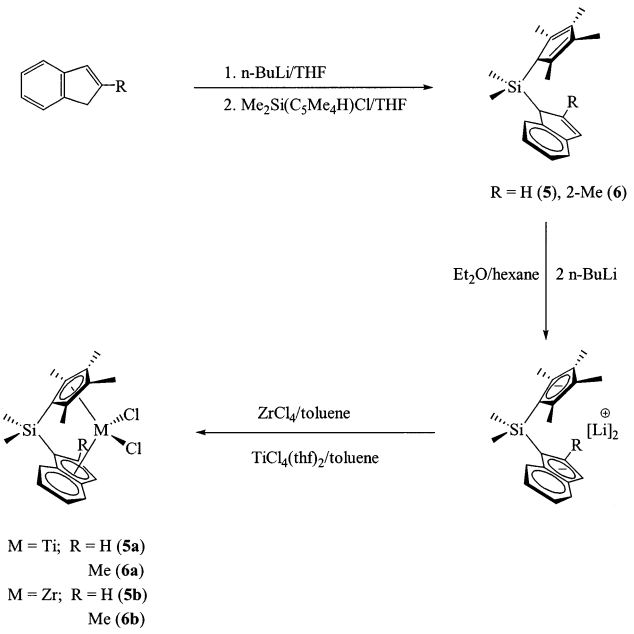

$TiCl_4(thf)_2$ and the dilithium salt obtained from the reaction of the corresponding ligand with 2 equiv of *n*-BuLi in a mixed solvent of diethyl ether and *n*-hexane at −78 °C. After workup and recrystallization, the final metallocenes were obtained as yellow crystalline solids for zirconium complexes (**5b** and **6b**) and dark green solids for titanium complexes (**5a** and **6a**) in moderate (∼40%) to low (∼25%) yields, respectively.

The molecular structures of three complexes, **5a**, **6a**, and **6b**, depicted in Figures 2, 3, and 4, respectively, reveal that there is no symmetry plane or axis in the molecule, showing the chiral C_1-symmetric nature irrespective of the type of metal and ligand. All the stereoisomers displayed in Figures 2, 3, and 4 have an *R*-configuration at C(1) according to the Cahn−Ingold−Prelog rules.[12] The metal centers are in a pseudotetrahedral coordination environment defined by the two chlorine atoms and by the two five-membered Cp rings.

Listed in Tables 2 and 3 are the summaries of the selected interatomic distances and angles, and the relevant geometrical parameters whose definitions are illustrated in Figure 5. The ring centroid−metal−ring centroid angles, designated as α in Table 3 and Figure 5, are in a normal range similar to those seen in other

(10) *MoleN*, An Interactive Structure Solution Program; Enraf-Nonius: Delft, The Netherlands, 1994.
(11) Sheldrick, G. M. *SHELXL 93*, Program for Crystal Structure Determination; University of Göttingen: Germany, 1993.
(12) Schlögl, K. *Top. Stereochem*. **1966**, *1*, 39.

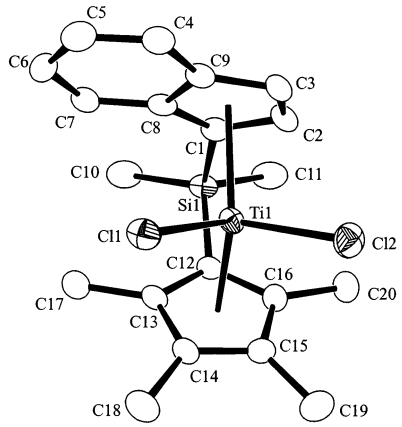

Figure 2. Molecular structure of $Me_2Si(C_5Me_4)(Ind)TiCl_2$ (**5a**). Thermal ellipsoids are drawn at the 35% probability level.

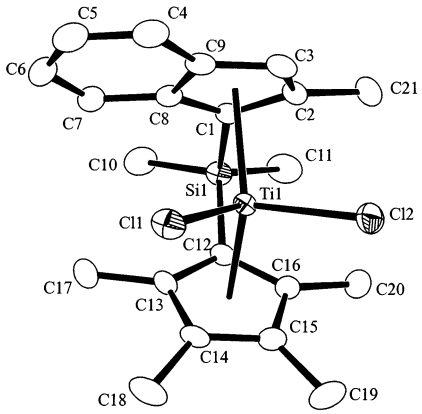

Figure 3. Molecular structure of $Me_2Si(C_5Me_4)(2\text{-}MeInd)TiCl_2$ (**6a**). Thermal ellipsoids are drawn at the 35% probability level.

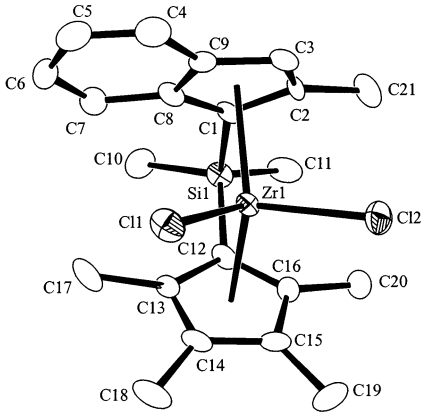

Figure 4. Molecular structure of $Me_2Si(C_5Me_4)(2\text{-}MeInd)ZrCl_2$ (**6b**). Thermal ellipsoids are drawn at the 35% probability level.

Si-bridged *ansa*-metallocenes.[5e,6f,13] Larger α values for titanium complexes **5a** and **6a** (131.5° and 131.4°, respectively) than that for zirconium complex **6b** (128.2°) indicate that the titanium atom is more tucked into the ligand envelope due to the smaller metal size. The decrease in metal size also induces the decrease of both the ring plane−ring plane dihedral angle (β value) and the bridging angle (ϕ value) noticeably. The larger α and smaller ϕ values for **5a**, **6a**, and **6b** than those in Chien's monocarbon-bridged systems $[MeHC(C_5Me_4)(Ind)]TiMe_2$ (127.0° and 105.4(9)°, respectively)[5b] and $[MeHC(C_5Me_4)(Ind)]ZrCl_2$ (118.2(1)° and 101.5(2)°, respectively)[4c] imply that the metal centers in the foregoing monosilicon-bridged complexes are significantly shielded by the *ansa*-ligand pocket, and thereby the exertion of efficient steric hindrance of the two ring fragments on the incoming α-olefin monomer and the polymer chain in the polymerization reactions may be expected.

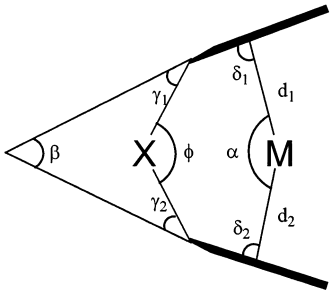

Figure 5. Scheme for the geometrical parameters.

The analysis of distances in Table 2 indicates that the interaction patterns between the metal center and the two five-membered rings in **5a**, **6a**, and **6b** are similar in a way that both the indenyl and the tetramethylcyclopentadienyl rings interact basically in a pentahapto fashion with a slightly longer metal−ring centroid distance (M−Cn(1)) for the indenyl ring fragment. The variation in the metal to ring carbon distances is somewhat larger for the indenyl ring than the tetramethylcyclopentadienyl ring.

Propylene Polymerizations. Propylene polymerizations with the catalytic precursors **5a**, **5b**, **6a**, and **6b** were carried out in the presence of MMAO cocatalyst at various reaction temperatures under 1 bar of propylene pressure. The polymerization data and the selected methyl sequence distributions of the resulting polypropylenes are given in Table 4 and Table 5, respectively.

Unlike the monocarbon-bridged $[MeHC(C_5Me_4)(Ind)]MCl_2$ systems,[4c,5a−c] all the metallocenes reported in this paper are found to be very active in propylene polymerization. The increased bridge length and the concomitant subtle changes in bonding geometry around the metal centers, observed in the molecular structures of **5a**, **6a**, and **6b**, appear to facilitate monomer incorporation into the growing polymer chain. It was also found by Collins et al. that monosilicon-bridged C_1-symmetric catalysts $[Me_2Si(Cp)(Ind)]MCl_2$ (M = Zr, Hf) are slightly more active than monocarbon-bridged ones.[5e]

The activity of both titanocenes **5a** and **6a** increases rapidly with decreasing temperature from 25 to −20 °C, while that of zirconocenes **5b** and **6b** increases with increasing temperature. This kind of reverse trend of temperature dependence of the polymerization activity is consistent with the results observed in other *ansa*-metallocenes.[14] It is generally accepted that the titanium system is more sensitive to the reaction temperature than the zirconium system, resulting in facile

(13) Spaleck, W.; Antberg, M.; Rohrmann, J.; Winter, A.; Bachmann, B.; Kiprof, P.; Behm, J.; Herrmann, W. A. *Angew. Chem., Int. Ed. Engl.* **1992**, *31*, 1347.

(14) The activity trend is intrinsically involved with the different insertion rate between Ti and Zr (Ti > Zr) according to decreasing M−C σ-bond strengths: Cardin, D. J.; Lappert, M. F.; Raston, C. L. In *Chemistry of Organo−Zirconium and −Hafnium Compounds*; Eds.; John Wiley and Sons: New York, 1986; p 16.

Downloaded by CARLI CONSORTIUM on June 29, 2009
Published on May 24, 2003 on http://pubs.acs.org | doi: 10.1021/om020712t

Table 5. Selected ^{13}C NMR Methyl Sequence Distributions of Polypropylenes Obtained with 5a, 5b, 6a, and 6b[a]

entry	mmmm	mmmr	mmrr	mrrm	mm	mr	rr	m	r	2rr/mr	4mm·rr/mr^2
1	0.717	0.127	0.117	0.039	0.844	0.117	0.039	0.903	0.097	0.67	9.62
2	0.827	0.078	0.076	0.019	0.905	0.076	0.019	0.943	0.057	0.50	11.91
3	0.881	0.052	0.045	0.022	0.933	0.045	0.022	0.956	0.044	0.98	40.55
4	0.700	0.129	0.128	0.043	0.829	0.128	0.043	0.893	0.107	0.67	8.70
5	0.817	0.079	0.068	0.036	0.896	0.068	0.036	0.930	0.070	1.06	27.90
6	0.759	0.105	0.099	0.037	0.864	0.099	0.037	0.914	0.086	0.75	13.05
7	0.176	0.161	n.d.[b]	n.d.	0.547	0.280	0.173	0.687	0.313	n.d.	n.d.
8	0.694	0.127	0.127	0.052	0.821	0.127	0.052	0.885	0.115	0.82	10.59
9	0.911	0.038	0.036	0.015	0.949	0.036	0.015	0.967	0.033	0.83	43.94
10	0.640	0.156	0.139	0.064	0.796	0.139	0.064	0.866	0.134	0.92	10.55
11	0.788	0.083	0.091	0.038	0.871	0.091	0.038	0.917	0.083	0.84	15.99
12	0.770	0.092	0.096	0.042	0.862	0.096	0.042	0.910	0.090	0.88	15.71

[a] Triad and dyad fractions were calculated from the corresponding pentad distributions. [b] n.d., not determined.

deactivation of a cationic active center, possibly due to reduction to Ti(III), at high temperature.[2a,15] In fact, above 50 °C the titanocenes gave little polymeric materials. The extremely high activity (>20 000 kgPP/(mol of Ti)·h·bar!) of the titanocenes at −20 °C can also be partially attributed to the increased stability of the cationic active centers as well as the increased monomer concentration at low temperature. A similar activity increase was also observed in Chien's catalyst (**1**).[5c] On the other hand, zirconocenes **5b** and **6b** show a general activity trend, indicating the increased reactivity of the cationic metal centers at higher temperature. The introduction of a methyl group at the 2-indenyl ring of C_1-symmetric metallocenes led to a decrease in the polymerization activity except at 0 °C for the zirconium system. This type of 2-Me effect is in good agreement with the result shown in C_2-symmetric *ansa*-zirconocenes.[13,16] The increased electron density at the cationic metal centers, which in turn can stabilize the active centers, appears to reduce the rate of polymerization.

The molecular weight of the polypropylenes increases with decreasing the reaction temperature in all cases, as generally observed in the polymerization of α-olefins catalyzed by metallocene complexes. Interestingly, the temperature dependence of the molecular weight of the polypropylene is larger in the titanocenes than in the zirconocenes. The molecular weight of the polypropylenes produced by titanocenes **5a** and **6a** at −20 °C (entries 3 and 9) is abnormally high, and in particular, the molecular weight of the polypropylene by **5a** (entry 3) exceeds 10^6, indicating the feature of ultrahigh-molecular weight polypropylene. 2-Me-substituted zirconocene **6b** gives polypropylenes with higher molecular weight than unsubstituted **5b** does at all temperatures, which is in accordance with the observations in the C_2-symmetric *ansa*-zirconocenes in which the 2-Me group on the indenyl ring suppresses the β-H elimination process.[16] However, in the case of the titanocenes, this trend is reversed, namely, the more active unsubstituted **5a** generates higher molecular weight polypropylenes at all temperatures. All the polypropylenes also have narrow molecular weight distributions (M_w/M_n) typical for polymerization by single-site catalysts.

To investigate the possible stereocontrol in the given C_1-symmetric *ansa*-metallocene systems, analyses of the methyl region in the ^{13}C NMR spectra of all polypropylenes were accomplished and the results are summarized in Table 5. The most striking feature is the microstructure of polypropylenes. All polypropylenes show moderate to high isotacticity: the methyl pentad [mmmm] content ranges from 64% to 91% except for the polypropylene by **6a** at 25 °C, which gives a low istotactic pentad value (entry 7). The titanium and zirconium systems show different temperature dependence of isotacticity. For the titanocenes, contrary to the result observed for Chien's monocarbon-bridged complex **1**,[5d] the isotacticity of the polypropylenes increases largely with decreasing reaction temperature as usually observed in other *ansa*-metallocene catalysts, while that of the polypropylenes by the zirconocenes does not follow this trend. Both zirconocenes afforded polypropylenes with a maximum isotacticity at 25 °C. In particular, titanocenes **5a** and **6a** gave highly isotactic polypropylenes ([mmmm] ≈ 90%) at −20 °C. This result is much different from those reported in similar C_1-symmetric *ansa*-metallocenes such as [MeHC(C_5Me_4)(Ind)]MCl_2 and [Me_2X(C_5H_4)(Ind)]MCl_2 (X = C, Si; M = Ti, Zr, Hf), which normally afforded polypropylenes with low [mmmm] content and thereby often produced elastomeric polypropylenes.[5a−f] In addition, in contrast to the increased stereoregularity of polypropylene upon 2-Me substitution at the indenyl ring in C_2-symmetric *ansa*-zirconocene complexes,[16] 2-Me substitution in the C_1-symmetric *ansa*-metallocenes systems led to lower stereoregularity at high temperatures. The melting temperature (T_m) of the polypropylenes increases with the increase of isotacticity as expected.

From the results described above, therefore, it can be suggested that the stereocontrol in the present C_1-symmetric catalysts will occur in the manner analogous to those suggested by Rieger[6c,d] and Chien and Rausch[6a,b] in their ethylene- and/or silicon-bridged fluorenyl-indenyl C_1-symmetric catalytic systems. Of two diastereotopic binding sites **A** (isospecific site) and **B** (aspecific site) relevant to our catalytic systems, depicted in Figure 6, the bulky polymer chain resides preferentially at the more open and thereby sterically less congested coordination site **B** to form a dominant state of an active species (state **I**). Then, the coordination of the incoming monomer at site **A** (state **II**) followed by chain migratory insertion would result in isospecific propagation with the formation of state **III**. However, the polymer chain

(15) Ewen, J. A. In *Catalytic Polymerization of Olefins*; Keii, T., Soga, K., Eds.; Kodansha: Tokyo, 1986; pp 271−292.
(16) Stehling, U.; Diebold, J.; Kirsten, R.; Röll, W.; Brintzinger, H. H.; Jüngling, S.; Mülhaupt, R.; Langhauser, F. *Organometallics* **1994**, *13*, 964.

Downloaded by CARLI CONSORTIUM on June 29, 2009
Published on May 24, 2003 on http://pubs.acs.org | doi: 10.1021/om020712t

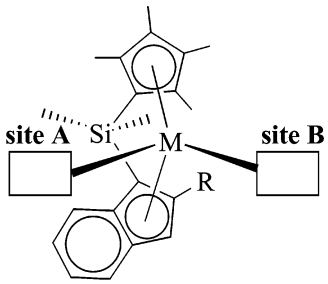

Figure 6. Schematic drawing of two diastereotopic binding sites **A** (isospecific site) and **B** (aspecific site) of $Me_2Si(C_5Me_4)(2\text{-R-Ind})MCl_2$.

in the resulting state **III** resides at site **A** and experiences steric hindrance from both the β-Me group of the C_5Me_4 ring and β-CH of the indenyl ring. To minimize this, the polymer chain would rapidly return to the sterically favorable state **I** via site isomerization, providing the new basis for the isotactic propagation with the state sequence of **I** → **II** → **III** → **I**. At which time, if a new monomer coordinates at the site **B** of state **III** before site isomerization occurs, then the ensuing chain migratory insertion will be nonstereoselective and thus will result in isolated [rr] stereoerrors. A methyl pentad distribution of [mmmr]:[mmrr]:[mrrm] ≈ 2:2:1 for moderate to high isotactic polypropylenes ([mmmm] > 64%) in Table 5 supports this formation of [rr] triad stereoerrors. The isotactic [mmmm] content in polypropylenes from zirconocenes at 25 °C is slightly higher than that at 0 °C, consistent with the observation that the combined effect of decreased monomer concentration and elevated temperature gives rise to more rapid site isomerization than monomer coordination.[6d] The reason for the decrease in [mmmm] content at 50 °C compared with that at 25 °C is not still clear but may include usual enantiofacial misinsertion that is favored at higher temperature and the chain epimerization process that is favored at lower monomer concentration as observed in C_2-symmetric *ansa*-metallocene catalysts.[17] On the other hand, the temperature dependence of the isotacticity for the titanocenes does not correspond exactly with that for the zirconocenes. The more tucked-in structure of the titanocenes than the zirconocenes appears to not only increase face selectivity of the incoming monomer during aspecific propagation but also facilitate site isomerization of the polymer chain at low reaction temperature due to the increased steric hindrance from both ring fragments.

The foregoing polymerization behavior of the present monosilicon-bridged complexes is obviously different from that of Chien's monocarbon-bridged C_1-symmetric catalyst system[4c,5a−d] despite their structural similarity. The formation of hemiisotactic polypropylene from both Chien's zirconium analogue of **1**[4c] and Razavi's [*i*-Pr(Flu)(3-MeCp)$ZrCl_2$][7] catalyst that contain a monocarbon bridge further supports that a bridging group can play an important role in controlling the microstructure of polypropylene obtained from the C_1-symmetric catalysts having a similar ligand environment. It can be thus concluded that the increased bridge length of an *ansa*-ligand by which the metal center can be effectively shielded influences significantly the propylene polymerization reactions in terms of both activity and selectivity.

Acknowledgment. Financial support from the Korea Science and Engineering Foundation (R02-2002-000-00057-0) is gratefully acknowledged.

Supporting Information Available: Crystallographic data for **5a**, **6a**, and **6b**. This material is available free of charge via the Internet at http://pubs.acs.org.

OM020712T

(17) (a) Busico, V.; Cipullo, R. *J. Am. Chem. Soc.* **1994**, *116*, 9329. (b) Busico, V.; Cipullo, R. *J. Organomet. Chem.* **1995**, *497*, 113. (c) Yoder, J. C.; Bercaw, J. E. *J. Am. Chem. Soc.* **2002**, *124*, 2548.

Downloaded by CARLI CONSORTIUM on June 29, 2009
Published on May 24, 2003 on http://pubs.acs.org | doi: 10.1021/om020712t